Advanced Journal of Chemistry-Section A

Journal homepage: www.ajchem-a.com

Review Article

Metal Organic Frameworks (MOFs) and their Application as Photocatalysts: Part II. Characterization and Photocatalytic Behavior

Mohammad Sajjadnejad [1]*, Seyyed Mohammad Saleh Haghshenas [2]

[1] *Department of Materials Engineering, School of Engineering, Yasouj University, Yasouj, Iran*
[2] *Department of Materials Science and Engineering, Shiraz University, Shiraz, Iran*

ARTICLE INFO

Article history

Submitted: 12 March 2023
Revised: 11 April 2023
Accepted: 16 April 2023
Available online: 16 April 2023
Manuscript ID: AJCA-2303-1357
Checked for Plagiarism: Yes

DOI: **10.22034/AJCA.2023.389622.1357**

KEYWORDS

Metal-organic-framework (MOF)
Nanocomposite
Porosity
Surface area
Photocatalysis

ABSTRACT

In recent years, metal-organic-frameworks (MOFs) have been increasingly considered as a new category of noble nanomaterials and received remarkable attention and attained great importance due to their superior properties such as high porosity and the specific surface area, adjustable organic linkers- metal clusters connections to use in multifunctional applications such as using as semiconductor, catalyst, drug delivery, gas separation, absorption, chemical production, catalysis, and photocatalysis in photochemical hydrogen evolution for water splitting, CO_2 reduction, and organic reactions fields for specific applications like adsorption and gas separation, hydrogen and CO_2 absorption, catalysis, photocatalysis, and biocompatibility. In comparison with aluminosilicates (zeolites, periodic mesoporous organosilica (PMOs), and other porous solids, MOFs as new advanced and novel photocatalysts are becoming multifunctional promising nanomaterials with impressive results, depicting a bright future of applications for great purposes, such as semiconductors, photo-responsive and photocatalysts materials employed in photochemical hydrogen evolution for water splitting (water oxidation), CO_2 reduction, heterogeneous catalysis, and organic reactions fields.

GRAPHICAL ABSTRACT

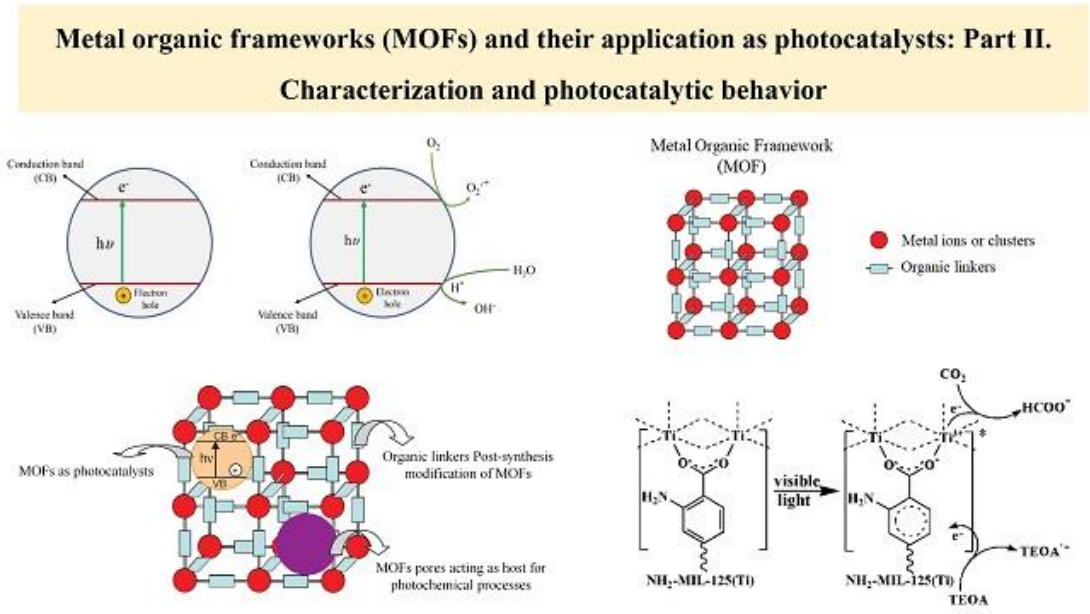

* Corresponding author: Sajjadnejad, Mohammad
✉ E-mail: m.sajjadnejad@yu.ac.ir ; m.sajjadnejad@yahoo.com

Introduction

In recent years, Metal-organic-frameworks (MOFs) as a new group of compounds with high porosity [1], significant specific surface area, crystallinity [2], tenability, structural tunability [3], diversified compound structure [4], and controllable pore size compared to prevalent semiconductors, have been increasingly recognized as an encouraging category of promising advanced materials with outstanding performance for versatile applications presenting excellent performances in fields containing drug delivery and medicine [5, 6], gas separation [7], wastewater purification [8-10], gas storage [11], adsorption [12], sensors [13], heat exchange [14], catalysis [15, 16], and photocatalysis [17-20]. MOFs have been recognized as a promising category of materials for photocatalytic applications due to their large surface area and porosity facilitating adsorption towards chemicals, tunable crystallinity and optical and electronic properties for efficient light absorption in the visible region, and finally, tunable composition and functionality that make them versatile photocatalysts for an extended range of reactions [17]. Formerly, in the first part of our review, "metal-organic frameworks (MOFs) and their application as photocatalysts", we tried to comprehensively review the structure, synthesis, post-synthesis, and purification of MOFs. In the second part of our review, "Metal Metal-organic frameworks (MOFs) and their application as photocatalysts", we have made considerable effort to emphasize the photocatalytic behaviour, characterization, and application of MOFs as photocatalysts.

Photocatalysis and application of MOFs

Photocatalysis is a promising technology that uses solar energy for energy regeneration and environmental remediation. In other words, it is a significant process of converting solar energy to chemical energy [21]. So, it is one of the most promising technologies with various renewable energy projects via new photocatalysts. TiO_2, Ag_3PO_4, WO_3, CdS, and ZnS are some of the most famous compound's categories that have illustrated great potential in the photolysis of water to produce hydrogen fuel, decomposition or decomposition oxidization of hazardous compounds and photoelectron chemical conversion. New photocatalyst materials have attracted significant attention in research in recent years [22].

Most organic photochemistry studies were performed in homogeneous gas and liquid phases in the first days. According to high energy electronically excited states, chemical and physical routes can occur extensively about light excitation of organic molecules. Therefore, a molecule can deactivate by emitting a photon of longer wavelength (lower energy) than the one applied for excitation (fluorescence and phosphorescence) or can undergo rearrangement, which causes chemical transformations and hardening production of a single product by photochemical reactions and producing a few compounds due to radiationless deactivation of excited states [23, 24]. Although light absorption is a universal phenomenon that occurs virtually in every organic molecule, homogenous photochemistry has not been employed as a favorite synthetic process in contrast to thermal activation [25]. Single-site heterogeneous catalyst is a catalyst constituted by a single metal center, which meansa metal ion, atom, or small cluster of atoms kept by surface ligands to a rigid framework. These single sites are isolated inside the hosting structure [26].

MOFs can serve as single-site photocatalysts and hold the advantage of the solid nature of MOF catalysts to facilitate recovery and use highly costly photocatalysts again by reducing contamination by the photocatalysts, which usually consist of heavy metals. Among the favorite materials to perform the photochemical reactions of incorporated guests, porous solid

materials are suitable for photochemistry in heterogeneous media [27]. The 3D structures of four groups of porous solids are demonstrated in Figure 1.

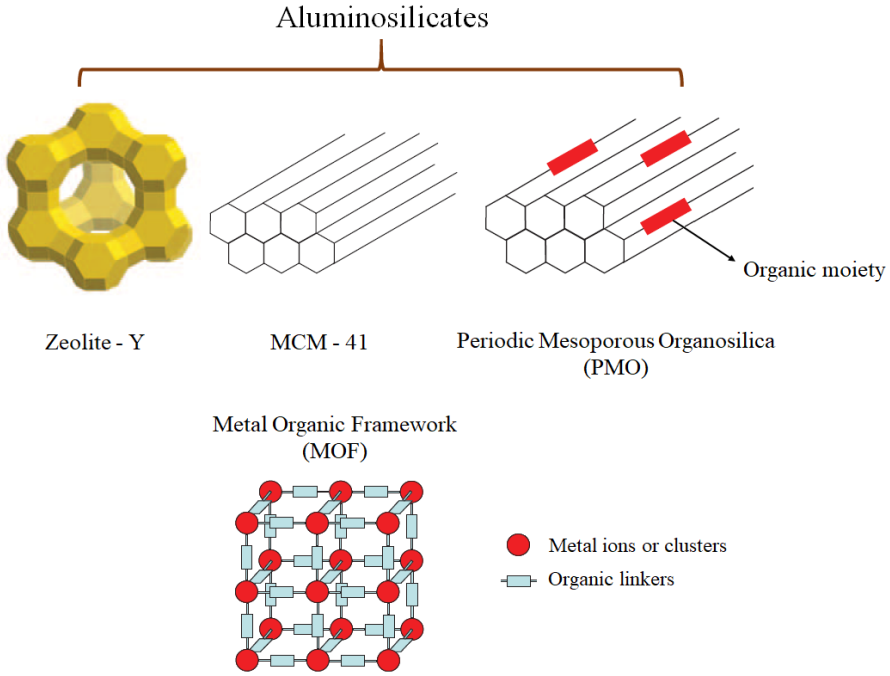

Figure 1. 3D structures of four different porous solids [28]

According to the four porous structures shown in Figure. 1, using a porous matrix is highly important to provide a rigid cavity in which permitting the mass transfer and incorporation inside of the crystals of a photoactive guest can be performed that causes photo-excitation, and finally, a photochemical reaction occurs. In fact, in the case of many of these porous solids, light excitation induces an electron transmission from the negative non-metallic element (sulfide or oxide) to the transition metal cation by producing a positive electron hole in the non-metallic element and an electron confined to the transition metal cation with various energies.

In solids with a high degree of crystallinity, a not much conductive band gap is called the valence band (VB), and a conductive band in which an electron can move throughout the material and this band is called the conduction band (CB). These solids show a semiconductor behavior in which before irradiation and light excitation, they behave like an isolator, but by irradiation, the electron transmitted and diffused to the conduction band induces the material to a conductive material. Due to charge transmission to the outer surface of the material, electrons and electron holes can react with organic compounds, which causes the same particle to behave as an oxidizing (electron hole in the valence band) and reducing agent (electrons in the conduction band) at the same time, with different redox potential depending on the situation of the valence and conduction bands [28].

The semiconductor behavior phenomenon in a semiconductor is schematically presented in Figure 2a. Upon absorbing a photon with higher energy than the valence-conduction band gap. Many commonly employed photocatalysts possess too wide bandgaps (3–3.4 eV) to harness visible light and a very low surface area for efficient production.

For the photocatalysis process in an environment like an atmosphere and in the presence of water, semiconductor behavior

differs from the simple schematic in Figure 2-a. In fact, in the atmosphere, by considering the oxygen electron acceptance ability, semiconductor irradiation in the air causes the production of superoxide (O_2^-) and species derived from it that are noted as reactive oxygen species (ROS). For the irradiations applied in water, this molecule can act as a hole quencher, leading to a proton and the formation of highly aggressive hydroxyl radicals, which is also considered one case of ROS. In Figure 2-b, some general processes schematically shown can be performed by electrons reaction in the conduction band with oxygen and positive holes in the valence band with water. According to Rauf *et al*. in 2011 [29], the possibility of all reactions in photocatalysis processes in the presence of TiO_2 is greatly attributed to the presence of both dissolved oxygen and water molecules. Without these two, the highly reactive hydroxyl radicals (OH•) could not be formed, preventing the photodegradation of liquid-phase organic molecules.

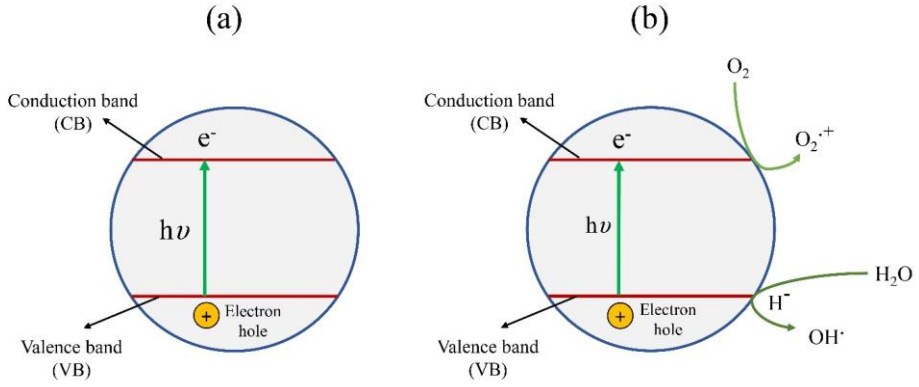

Figure 2. Schematic mechanism of semiconductor behavior. a) semiconductor phenomenon upon absorbing a photon with higher energy than the valence-conduction band gap. b) semiconductor acting simultaneously as oxidizing (the positive hole) and reducing (electrons in the conduction band) agent.

Despite MOFs' remarkable advantages and superior properties as photocatalysts, some restrictions limit their use in photocatalytic applications, such as low conductivity and stability and extensive electron-hole pair recombination [30]. Thus, various strategies better be applied to enhance the photocatalytic application potential of these materials, such as the formation of a heterojunction with a narrow band gap semiconductor, the insertion of an amino group in the organic linker, and the introduction of a MOF, backbone [31]. Two-dimensional (2D) materials have received considerable attention as promising semiconductors for forming a heterojunction to develop more efficient photocatalysts with high charge-carrier mobility and current stability, thermal stability, and conductivity [32]. They could be classified as a group of materials having layered structures, including many organic, inorganic, and hybrid materials, such as graphene, graphite, graphitic carbon nitride (g-C_3N_4), specific transition metal oxides, transition-metal-dichalcogenides (TMDs, such as MoS_2, TiS_2, TaS_2, WS_2, $MoSe_2$, and WSe_2) and other semiconductors [33-35]. The superior physical and chemical properties of 2D photocatalysts make them different from other materials due to their layered structure with a high specific surface area due to in-plane chemical bonds and van der Waals forces between the layers [32, 35].

In MOFs, the organic linker acts as VB, and the metallic cluster plays the role of CB. Remarkably, the process for an organic semiconductor is also

described as occurring between the highest occupied molecular orbital (HOMO) and the lowest unoccupied molecular orbital (LUMO) [36-38].

In recent years, TiO_2 has been widely utilized as a well-studied and highly useful photocatalyst [39-49] and semiconductor [50-53]. Although MOF, as a new multifunctional material type introduced recently by researchers, can be an excellent and suitable alternative material as a semiconductor [54]. TiO_2 in the anatase form is the most critical photocatalyst. Its presence in different forms significantly influences the structure of the MOF metal clusters core and its connection to the linkers. For example, MIL125 MOF is an actual example of a photoactive metal cluster consisting of a cyclic octamer of edge and corner-sharing TiO_5 octahedral connected by BDC ligands. An efficient photoinduced charge dissociation between the $Ti_8O_8(OH)_4$ units and the linker is established. The metal-to-ligand interaction develops in 3D space, defining empty spaces, indicated as cages, which causes getting access into the smaller channels [55].

According to the photocatalytic application's structure of MOFs, an organic compound linker may make MOFs more adaptable to many functions than zeolites. Generally, pure zeolites and aluminosilicates do not absorb UV radiations of wavelengths longer than 220 nm. A famous MOF (MOF-5) has an absorption spectrum with an onset at 450 nm. Thus, this MOF can be encountered with photochemical processes upon photoexciting the organic linker [56].

The intimate connection of organic linkers with metal clusters can significantly affect the sensitivity of metal clusters caused by the organic linkers, a basic phenomenon termed the “antenna effect” [28]. The antenna effect is attributed to MOFs with rare earth metal compounds such as Lanthanum coordination compounds and their metal clusters' sensitivity to organic linkers for photoluminescence application [57-59]. Allendorf *et al*., in 2009 [57], reported the critical role of the linker in MOF luminescence, in which, for example, lanthanide-based luminescence typically requires an antenna molecule in the framework for energy transfer.

Today, MOFs are the most porous materials, possessing an extensive surface area and too high internal pore volume due to the metal-ligand interaction's directionality and the organic linkers' low weight. For instance, Zeolites, as a famous substance, has a specific surface area value of 400 m^2g^{-1} or below and pore volumes of 0.2 cm^2g^{-1} or smaller. Periodic mesoporous aluminosilicates (PMAs) such as MCM-41 or SBA-15 can have a BET area over 1000 m^2g^{-1} and a pore volume of 0.5 cm^2 g^{-1}. MOFs have been reported highest porous structures, which possess a specific surface area above 5000 m^2g^{-1} and pore volumes above 1 $cm^2g^{-1,}$ and also the lowest framework density, weight per nm^3, which means the lowest ever reported [60].

The extremely wide-open structure of MOFs provides the free space available for host molecules reaching up to 90% of the crystal volume [61]. Due to the large surface area and pore volume, one of the main applications of MOFs is for utilization as absorbents for gas separation and as the stationary phase in liquid chromatography. Hydrogen and CO_2 absorption [62-64], and heterogeneous catalysts [65-67] are also regarded as other examples in which MOFs are beneficial materials for these applications.

In this regard, the porosity of MOFs provides a large and highly suitable surface area and accessibility of the substrates to fully accomplishment of photochemical reactions since linkers present visible absorption bands that can photosensitize the small metallic clusters causing efficient charge separation.

Developing efficient MOFs as photocatalysts and decreasing the semiconductor particle size induces a limitation concerning MOFs structures with isolated clusters of semiconducting quantum dots. Therefore, a limitation is induced

due to some of the metal clusters' structural nodes, which leads to the reduction of metal atoms to the minimum possible number and also the assurance of no agglomeration of quantum dots possibility is achieved by the linker. Thus, the linker could play two roles as an antenna, isolating the semiconducting quantum dots, absorbing light of the appropriate wavelength, and transmitting energy to the non-absorbing quantum dot. In this regard, the MOF structure will be appropriated as a photocatalyst due to good absorption bands by the ability of linkers and the metallic clusters to act as quantum dots. A photocatalyst has to merge some of the essential characteristics of a catalyst, such as high surface area and single site composition, with other specific essential properties for an appropriate light interaction, like effective photophysical processes, an adequate absorption spectrum, and long lifetime of excited states [28].

MOFs Photochemical Activity

To develop photoactive materials based on MOFs, three general approach classification [28, 68] are shown schematically in Figure 3.

In the first approach, MOF can be used as a porous 3D matrix to confine a chromophore responsible for the photochemical properties. A chromophore is a molecule part responsible for its color. In fact, in this strategy, the MOF structure matrix and porosity positions play a key role by producing a reaction cavity in which the reaction occurs for photochemical activity. Thus, the chromophore is isolated due to the MOF rigid structure. This rigid structure can also immobilize and induce intramolecular events. This strategy still needs modification for MOFs because it is also observed for reported zeolites and other microporous and mesoporous porous solids [28].

In the second approach, the semiconducting quantum dots properties will be used and derived from the metallic clusters' existence [54]. In this strategy, charge separation occurs due to the light absorption on the organic linker by creating an electron in the metal cluster and a hole in the the electron-rich linker. This charge separation also occurs in most semiconductors and can transform light into chemical energy [69, 70].

And finally, in the third approach, MOFs organic linkers are modified. They will be converted into photo-responsive units after the synthesis process (post-synthetic modification), or the MOFs will be synthesized by photo-responsive organic ligands [71-73]. Due to the high photochemistry propensity of most organic groups, this approach can be applied to develop whole categories of photo-responsive solids with the application as sensors in photoluminescence, photochromics, and other applications based on the organic compounds' inherent activity [28].

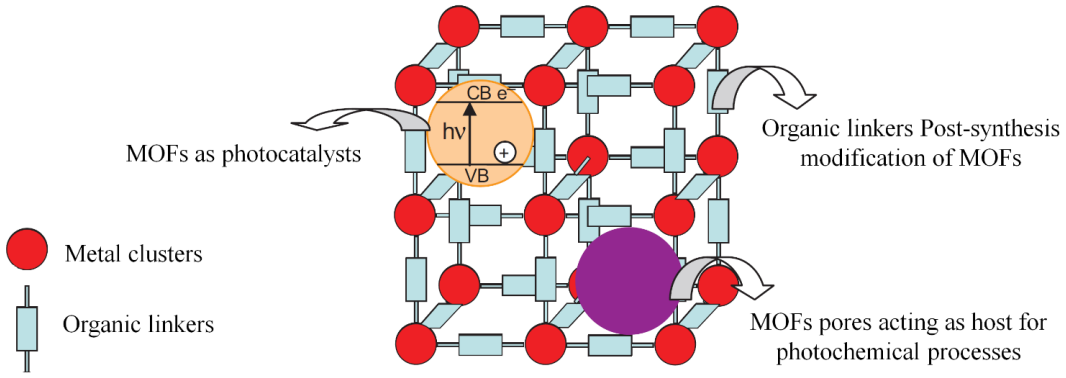

Figure 3. Different strategies for developing photoactive materials based on MOFs

MOFs as Photocatalysts

Due to the presence of catalytically active metals and functional organic linkers, the easily tailorable physical and chemical functions, together with the large surface area and permanent pores/channels to potentially anchor/encapsulate photosensitizers and catalytic moieties, MOFs hold and have already shown great opportunities for heterogeneous photocatalysis to operate artificial photosynthetic reactions including water splitting [4, 5], CO_2 reduction [6-8], and organic photosynthesis [9, 10]. Nowadays, using of MOFs as photo-catalysts has increased dramatically.

The first study of a MOF as a photo-catalyst to degrade organic pollutants was reported by Mahata *et al*. in 2006 [18]. Garcia *et al*., in 2007 [56, 74], investigated the photocatalytic properties of MOF-5(Zn) in phenol degradation and demonstrated that MOF-5 showed reverse shape-selectivity. They found that the terephthalate linkers could absorb light and sensitize the semiconductor dots.

In 2008 [69], Gascon *et al*. studied the influence of organic linkers on the photocatalytic activity of MOF-5. It has been shown that changing the organic linker can adjust the band gap energy of MOFs shown in Figure 4. Their results showed that naphthalene-dicarboxylic acid as a linker performed the best catalytic activity in the photooxidation of propene [69].

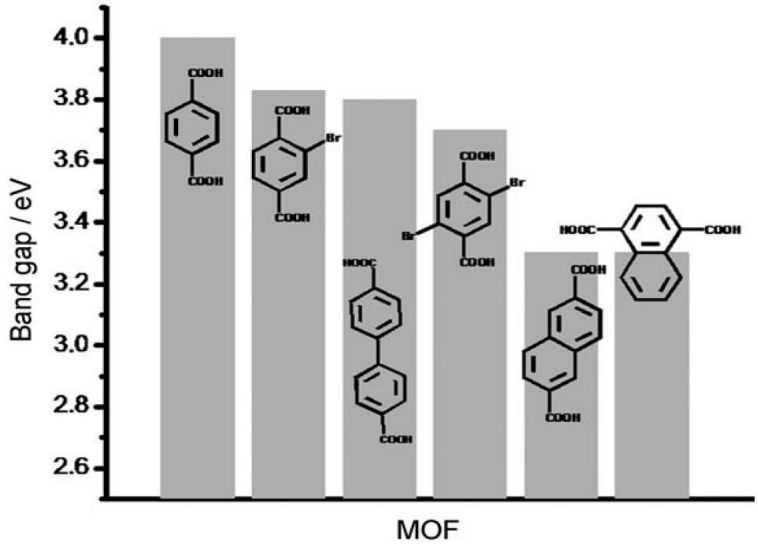

Figure 4. The band gap value of different MOF linkers [69]

Dan-Hardi *et al*., in 2009 [55], synthesized MIL-125(Ti) for the first time. A high photonic sensitivity was observed from this hybrid MOF substance for forming Ti(III)-Ti(IV) mixed valence under UV-visible irradiation in the presence of alcohols and titanium centers, and oxidation-reduction of absorbed alcohol molecules happened at the same time. A recent study done by George *et al*. in 2017 [75] on this MOF type (MIL-125(Ti)) which was quickly synthesized by a microwave technique, resulted in possessing a band gap energy of 3.14 eV that could degrade MB to ca. 96.77% in 6 h under UV-light irradiation.

The first study on UiO-66, an ordinarily water-tolerant Zr–containing MOF, was done by Xamena et al. in 2010 [76]. Later studies were done on this MOF type in the visible-light-driven photocatalytic degradation of MO (Methyl Orange) [77] and degradation of MB (Methylene Blue) under UV-light irradiation [78].

Li et al. in 2012 [79], investigated amine-functionalized Ti-based porous MOF (NH_2-MIL-125(Ti) ($Ti_8O_8(OH)_4(NH_2\text{-}BDC)_6$, BDC = benzene-1,4-dicarboxylate) as an efficient photocatalyst for CO_2 reduction under visible-light irradiations [38]. The MOF showed a visible absorption band that extends to 550 nm due to enhancing the amino group. During the photocatalytic reaction, CO_2 was reduced into HCO_2^- photochemically in acetonitrile with triethanolamine (TEOA) as the sacrificial reducing agent, as seen in Figure 5. It was suggested that an endured charge transfer excited state was created and reduced by TEOA to give a Ti^{3+} center which in turn caused a reduction of CO_2 to give HCO_2^-. NH_2-MIL-125(Ti) showed few photocatalytic activities for photochemical CO_2 reduction, with a TON of 0.03 per Ti attained within 10 h.

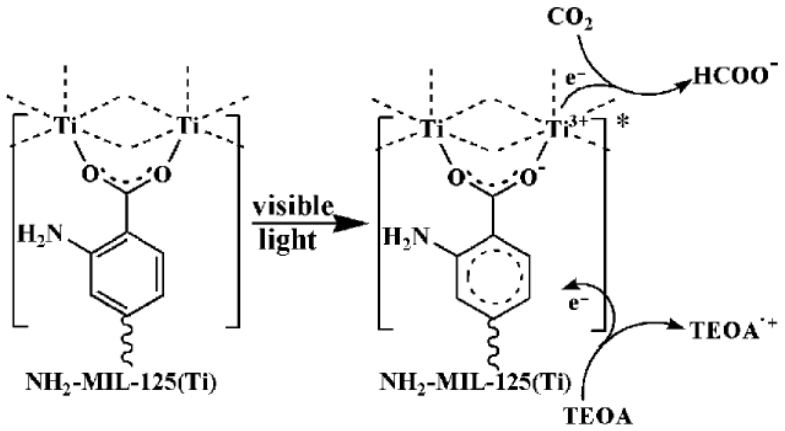

Figure 5. Proposed mechanism for the photocatalytic CO_2 reduction of NH_2-MIL-125(Ti) under visible light irradiation [79]

In 2014 [80], Zhang and Lin reviewed MOFs artificial photosynthesis and photocatalysis and focused on fundamental principles of energy transfer. Photocatalysis and the latest advancements of MOF applications in energy transfer, light-harvesting, CO_2 reduction, and water oxidation.

Mosleh *et al*., in 2016 [80], synthesized a new composite of mesoporous materials, HKUST-1 metal-organic framework, and SBA-15 and applied it to the simultaneously visible light photodegradation of a binary mixture of safranin O and malachite green. The photodegradation process was done in a rotating packed bed reactor (Figure 6) to increase mass transfer and irradiance distribution. Due to high rotational speed, thick liquid films are converted into thin layers and small droplets by creating a rigorous centrifugal field. Therefore, the interfacial area between pollutants and photocatalyst particles increases, and mass transfer is improved dramatically. They have attained optimum values for maximum efficiency using HKUST-1- BA-15 at an MG concentration of 10 $mg.L^{-1}$, SO concentration of 15 $mg.L^{-1}$, a rotational speed of 900 rpm, a solution flow rate of 0.4 $Lmin^{-1}$, HKUST-1-SBA-15 dosage of 0.25 $g.L^{-1}$, and irradiation time of 80 min. The maximum photodegradation percentages of MG and SO obtained were 98.8% and 88.7%, respectively.

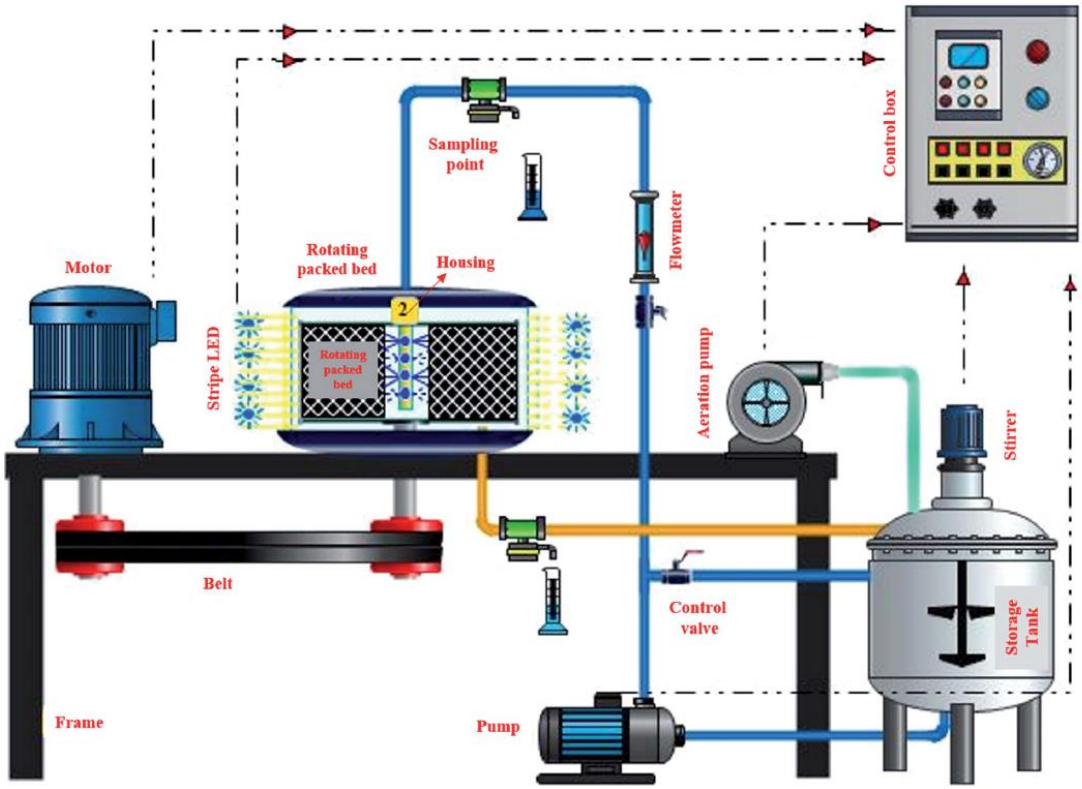

Figure 6. Rotating packed bed photocatalytic reactor schematic used for visible light photodegradation of a binary mixture of safranin O and malachite green [80]

Direct oxidative condensation between o-aminothiophenols and alcohols to produce 2-substituted benzothiazoles under visible light irradiations using O_2 as an oxidant over MIL-100(Fe) and MIL-68(Fe), two Fe-based MOFs were reported by Wang et al. [81], in which their study not only provided an economical, sustainable, and thus green process for the production of 2-substituted benzothiazoles but also proved the potential of using TAS to explain the activity data and perceive the photophysics of MOFs, that make them multifunctional catalysts as great alternatives for light-induced organic transformations.

Ramezanalizadeh and Manteghi, in 2018 [82], prepared MOF-based composite MOF/$CuWO_4$ with different weight ratios by an easily achieved route and assessed the photocatalytic performance of them for the degradation of methylene blue (MB) and 4-nitrophenol as water pollutions. They have concluded that the MOF/$CuWO_4$ composite with a weight ratio of (1:1) exhibited superior photocatalytic activity toward the degradation of the contaminants under LED light irradiation. Due to the MOF high surface area, efficient separation of electron-hole pairs was observed.

Thakare and Ramteke, in 2018 [83], reported a novel MOF-5 compound photocatalyst construction by interacting 8-Hydroxyquinoline with MOF-5 synthesized through a room temperature method. They have done the secondary complex formation between the Zn cluster with 8-Hydroxyquinoline to harness visible light and acted as a mediator to transfer photo-induced electrons to MOF-5 to enhance the photocatalytic reaction rate with visible light. They have validated their assert using photocatalytic phenol degradation as a representative organic pollutant under visible light irradiation.

Coupled TiO_2 nano-sheets and MOF (NH_2-UiO-66) were effectively used in an in-situ growth strategy to form bi-functional materials for the combined capture and photocatalytic reduction of CO_2 under UV-visible light irradiation by Crake *et al*. in 2018 [84], in which the improvement photoactivity to the enhanced abundance of long-lived charge carriers was observed as unveiled by transient absorption spectroscopy (TAS).

In 2019, Mahmoudi *et al*. [85] synthesized and characterized a metal-organic framework (MOF-199) as a nanoporous material using FESEM, EDS, FTIR, XRD, BET, and TGA. They utilized Basic Blue 41 for assessing the photocatalytic activity of MOF-199. The FESEM image in Figure 7, demonstrates that a nanoporous MOF was synthesized.

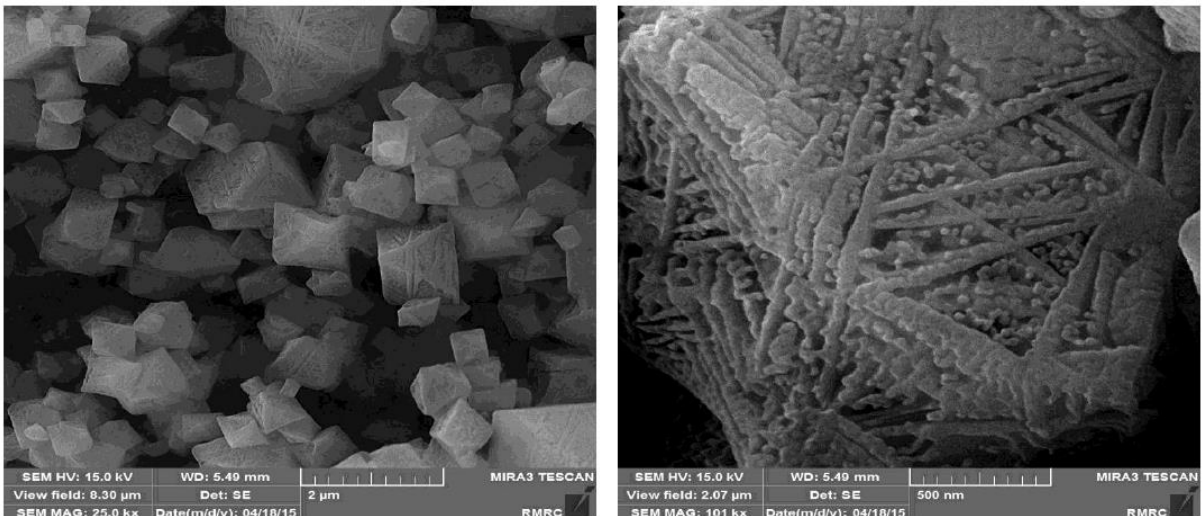

Figure 7. FESEM images of the synthesized nanoporous MOF-199 with different scales (a) 2 μm and (b) 500 nm [85]

Contaminant degradation was enhanced by increasing the catalyst dose, and it was lowered by initial dye concentration, so as the decolorization rate by diminishing the pH of the solution as a result of the electrostatic repletion of the cationic dye from the surface of MOF-199. Finally, their results proved the potential of the synthesized nanoporous metal-organic framework-199 as a photocatalyst for decolorizing wastewater.

MOFs can facilitate the development of composites with other semiconductors to generate Z-scheme heterojunctions that can effectively prevent the recombination of photogenerated charges. For instance, Chatterjee *et al*. in 2022 [17] constructed sensible Z-scheme heterojunctions in MOFs to mimic natural photosynthesis, providing MOF-based Z-scheme photocatalysts with higher light-harvesting capacity, spatially separated oxidative and reductive active sites, and well-preserved redox ability.

Due to the high specific surface area, high porosity of MOFs, and excellent visible light response of CdS, Jing *et al*. in 2022 [86] constructed the CdS/Cd-MOF nanocomposites by in-situ sulfurization to form CdS via Cd-MOF as precursor while the CdS loading controlled by the dose of thioacetamide. The larger specific surface area of the composite catalysts provided more active sites according to the higher degradation rate of methylene blue (MB) by 10 mg MOF/CdS-6 (mass ratio of MOF to thioacetamide was 6:1) was 91.9% in 100 min, which was higher than that of pure Cd-MOF (62.3%) and pure CdS (67.5%). Their Mott-

Schottky model experiment demonstrated effective inhibition of photogenerated electrons and hole recombination due to the generated type-II heterojunction between Cd-MOF and CdS. And finally, the MOF/CdS-6 illustrated good photocatalytic performance after five cycles, indicating outstanding stability and reusability.

Table 1. Pristine MOFs for photocatalysis and their corresponding applications

MOF types	Applications	Light source	Year	Ref.
MOF-5	Phenol degradation	UV	2007, 2008	[74, 89]
MOFs with changed linkers of MOF-5	Propylene oxidation	UV	2008	[69]
MIL-125	Alcohols oxidation, MB (Methylene Blue) degradation	UV	2009, 2017	[55, 75]
UiO-66	H_2 production	UV	2010	[76]
ZIF-8	MB (Methylene Blue) degradation	UV	2014	[78]
MIL-53(M) (M=Fe, Al, Cr)	MB (Methylene Blue) degradation	UV-vis, visible	2011	[38]
UTSA-38	MO (Methyl Orange) degradation	UV-vis	2011	[90]
Fe(III)-based MOFs	Rh6G degradation, O_2 production	Visible	2013, 2016	[91, 92]
NTU-9	RhB, MB (Methylene Blue) degradation	Visible	2014	[93]
MOFs with changed linkers of UiO-66	MO (Methyl Orange) degradation	Visible	2015	[77]
MIL-100, MIL-68	Benzene hydroxylation	Visible	2015	[94]
MIL-53 (Fe)	Cr(VI) reduction, dyes degradation and water oxidation	Visible	2015, 2017	[95-97]
ZIF-67	Cr(VI) reduction	UV-vis-NIR	2016	[98, 99]
MIL-100(M) (M = Al, Fe, V, Cr)	MB (Methylene Blue) degradation	UV	2016	[100]

Unique hybrid structures were constructed between a Ce-based MOF (Ce-MOF) and graphitic carbon nitride (g-C_3N_4) materials by Durmus *et al*. in 2023 [87], in which g-C_3N_4 materials were prepared by five various methods: conventional pyrolysis, chemical exfoliation by a strong acid, activation by an alkaline hydrothermal treatment, melamine-cyanuric acid supramolecular assembly with a mechanochemical method, and by the solvothermal pre-treated method. The structural and morphological properties of the resulting g-C3N4 sheets and their composites were also characterized via SEM, XRD, FTIR, TGA-DTG, UV–vis spectroscopy (UV–vis DRS), and N2 sorption-desorption isotherms (BET). The photocatalytic performance of the composites was assessed through the photocatalytic degradation of methylene blue (MB) in an aqueous solution under UV–visible light irradiation. Finally, the photocatalytic efficiency of the Ce-MOF/g-C3N4–TS composite was significantly higher than that of their counterparts (Ce-MOF or g-C3N4–TS) for the photocatalytic degradation of MB.

Table 1 shows MOFs for photocatalysts and their corresponding applications. These pristine MOF types of photocatalysts are rare and hard to adjust quickly. However, there are other modified MOFs than pristine form for photocatalysis, which has been well-studied and reviewed [88].

Conclusion and Remarks

This review article tried to cover several key conclusions emphasizing the importance of providing MOFs as a new approach to noble materials due to their unique well-ordered porous structure, high specific surface area, adjustable organic linkers- metal clusters connections to use in multifunctional applications such as using as semiconductor, catalyst, drug delivery, gas separation, absorption, chemical production, photocatalysis in photochemical hydrogen evolution for water splitting, CO_2 reduction, and organic reactions fields. The MOFs structure plays a crucial role in their unique properties, and an appropriate synthesis technique is employed to achieve the desired properties. It is concluded that MOFs, as a new advanced and novel photocatalyst, are promising multifunctional materials with impressive results, indicating a bright future as semiconductors, compared to aluminosilicates (zeolites, periodic mesoporous organosilica (PMOs) and other porous solids, photo-responsive and photocatalysts materials employed in photochemical hydrogen evolution for water splitting (water oxidation), CO_2 reduction, heterogeneous catalysis, and organic reactions fields.

Acknowledgment

The authors declare that no funds, grants, or other support were received during the preparation of this manuscript. Therefore no acknowledgments do apply.

Disclosure statement

The author reported no potential conflict of interest.

Orcid

M. Sajjadnejad: 0000-0001-5112-1791

References

[1] W. Meng, Y. Zeng, Z. Liang, W. Guo, C. Zhi, Y. Wu, R. Zhong, C. Qu, R. Zou, *Chem. Sus. Chem.,* **2018**, *11*, 3751–3757. [CrossRef], [Google Scholar], [Publisher]

[2] W. Tu, Y. Xu, S. Yin, R. Xu, *Adv. Mater.,* **2018**, *30*, 1707582. [CrossRef], [Google Scholar], [Publisher]

[3] J.D. Xiao, H.L. Jiang, *Acc. Chem. Res.,* **2018**, *52*, 356–366. [CrossRef], [Google Scholar], [Publisher]

[4] J.D. Xiao, L. Han, J. Luo, S.H. Yu, H.L. Jiang, *Angew. Chem., Int. Ed.,* **2018**, *57*, 1103–1107. [CrossRef], [Google Scholar], [Publisher]

[5] M. Pander, A. Żelichowska, W. Bury, *Polyhedron,* **2018**, *156*, 131–137. [CrossRef], [Google Scholar], [Publisher]

[6] C. Orellana-Tavra, R.J. Marshall, E.F. Baxter, I.A. Lázaro, A. Tao, A.K. Cheetham, R.S. Forgan, D. Fairen-Jimenez, *J. Mater. Chem. B,* **2016**, *4*, 7697–7707. [CrossRef], [Google Scholar], [Publisher]

[7] J.R. Li, J. Sculley, H.C. Zhou, *Chem. Rev.,* **2012**, *112*, 869–932. [CrossRef], [Google Scholar], [Publisher]

[8] O. Akeremale, *J. Chem. Rev,* **2022**, *4*, 1-14. [Google Scholar]

[9] V. Safarifard, Y. Davoudabadi Farahani, *J. Iran. Chem. Commun,* **2020**, *8*, 109–125. [Google Scholar]

[10] H. Shayegan, V. Safarifard, H. Taherkhani, M.A. Rezvani, *J. Iran. Chem. Commun.,* **2020**, *8*, 190–200. [Google Scholar]

[11] J. Flieger, M. Tatarczak-Michalewska, E. Blicharska, A. Madejska, W. Flieger, A. Adamczuk, *Sep. Purif. Technol.,* **2019**, *209*, 984–989. [CrossRef], [Google Scholar], [Publisher]

[12] Y.T. Dang, H.T. Hoang, H.C. Dong, K.B.T. Bui, L.H.T. Nguyen, T.B. Phan, Y. Kawazoe, T.L.H. Doan, *Micropor. Mesopor. Mater.,* **2020**, *298*, 110064. [CrossRef], [Google Scholar], [Publisher]

[13] L.E. Kreno, K. Leong, O.K. Farha, M. Allendorf, R.P. Van Duyne, J.T. Hupp, *Chem. Rev.,* **2012**, *112*, 1105–1125. [CrossRef], [Google Scholar], [Publisher]

[14] D. Lenzen, P. Bendix, H. Reinsch, D. Fröhlich, H. Kummer, M. Möllers, P.P. Hügenell, R. Gläser, S. Henninger, N. Stock, *Adv. Mater.,* **2018**, *30*, 1705869. [CrossRef], [Google Scholar], [Publisher]

[15] B.N. Bhadra, A. Vinu, C. Serre, S.H. Jhung, *Mater. Today,* **2019**, *25*, 88–111. [CrossRef], [Google Scholar], [Publisher]

[16] L. Zhu, X.Q. Liu, H.L. Jiang, L.B. Sun, *Chem. Rev.,* **2017**, *117*, 8129–8176. [CrossRef], [Google Scholar], [Publisher]

[17] A. Chatterjee, L. Wang, P. Van Der Voort, *Chem. Commun.,* **2023**, *59*, 3627–3654. [CrossRef], [Google Scholar], [Publisher]

[18] P. Mahata, G. Madras, S. Natarajan, *J. Phys. Chem. B,* **2006,** *110*, 13759–13768. [CrossRef], [Google Scholar], [Publisher]

[19] Q. Shang, Zeng, T., Gao, K., Liu, N., Cheng, Q., Liao, G., Pan, Z. and Zhou, H., *New J. Chem.,* **2019**, *43*, 16595–16603. [CrossRef], [Google Scholar], [Publisher]

[20] H. Fakhri, H. Bagheri, *Mater. Sci. Semicond. Process.,* **2020**, 107, 104815. [CrossRef], [Google Scholar], [Publisher]

[21] G. Liu, P. Niu, L. Yin, H.M. Cheng, *J. Am. Chem. Soc.,* **2012**, *134*, 9070–9073. [CrossRef], [Google Scholar], [Publisher]

[22] H. Zhang, G. Liu, L. Shi, H. Liu, T. Wang, J. Ye, *Nano Energy,* **2016**, *22*, 149–168. [CrossRef], [Google Scholar], [Publisher]

[23] M. Montalti, A. Credi, L. Prodi, M.T. Gandolfi *Handbook of photochemistry*, CRC press, **2006**. [Google Scholar]

[24] J.C. Scaiano, *CRC handbook of organic photochemistry*, CRC press, **1989**. [Google Scholar]

[25] L. Kaanumalle, A. Natarajan, V. Ramamurthy, *In Synthetic Organic Photochemistry (Molecular and Supramolecular Photochemistry)*; Griesbeck, AG; Mattay, J., Eds. Marcel Dekker: New York, **2005**.

[26] A. Zecchina, S. Bordiga, E. Groppo, *Selective Nanocatalysts and Nanoscience: Concepts for Heterogeneous and Homogeneous Catalysis,* **2011**, pp. 1-27 [Google Scholar]

[27] J. Mattay, *Photochemistry in Microheterogeneous Systems*. Von K. Kalyanasundaram, Academic Press: New York,

Angew. Chem., **1988**, *100*, p. 744. [Google Scholar]

[28] H. García, B. Ferrer, *Photocatalysis by MOFs*, **2013**, pp. 365–383. [CrossRef], [Google Scholar], [Publisher]

[29] M. Rauf, M. Meetani, S. Hisaindee, *Desalination,* **2011**, *276*, 13–27. [CrossRef], [Google Scholar], [Publisher]

[30] Z. Ding, S. Wang, X. Chang, D.-H. Wang, T. Zhang, *RSC Adv.,* **2020**, *10*, 26246–26255. [CrossRef], [Google Scholar], [Publisher]

[31] G. Liao, C. Li, X. Li, B. Fang, *Cell Rep. Phys. Sci.,* **2021**, *2*, 100355. [CrossRef], [Google Scholar], [Publisher]

[32] G. Algara-Siller, Severin, N., Chong, S.Y., Björkman, T., Palgrave, R.G., Laybourn, A., Antonietti, M., Khimyak, Y.Z., Krasheninnikov, A.V., Rabe, J.P. and Kaiser, U. *Angew. Chem., Int. Ed.,* **2014**, *53*, 7450–7455. [CrossRef], [Google Scholar], [Publisher]

[33] T. Su, Q. Shao, Z. Qin, Z. Guo, and Z. Wu, *ACS Catal.,* **2018**, *8*, 2253–2276. [CrossRef], [Google Scholar], [Publisher]

[34] C. Tan, X. Cao, X.J. Wu, Q. He, J. Yang, X. Zhang, J. Chen, W. Zhao, S. Han, G.H. Nam, M. Sindoro, , *Chem. Rev.,* **2017**, *117*, 6225–6331. [CrossRef], [Google Scholar], [Publisher]

[35] J. Low, S. Cao, J. Yu, S. Wageh, *Chem. Commun.,* **2014**, *50*, 10768–10777. [CrossRef], [Google Scholar], [Publisher]

[36] V. Coropceanu, J. Cornil, D.A. da Silva Filho, Y. Olivier, R. Silbey, J.L. Brédas, *Chem. Rev.,* **2007**, *107*, 926–952. [CrossRef], [Google Scholar], [Publisher]

[37] L. Kaake, P.F. Barbara, X.Y. Zhu, *J. Phys. Chem. Lett..* **2010**, *1*, 628–635. [CrossRef], [Google Scholar], [Publisher]

[38] J.J. Du, Y.P. Yuan, J.X. Sun, F.M. Peng, X. Jiang, L.G. Qiu, A.J. Xie, Y.H. Shen, J.F. Zhu, *J. Hazard. Mater.,* **2011**, *190*, 945–951. [CrossRef], [Google Scholar], [Publisher]

[39] J. Bandara, C. Hadapangoda, and W. Jayasekera, *Appl. Catal. B,* **2004**, *50*, 83–88. [CrossRef], [Google Scholar], [Publisher]

[40] V.N.H. Nguyen, R. Amal, D. Beydoun, *Chem. Eng. Sci.,* **2003**, *58*, 4429–4439. [CrossRef], [Google Scholar], [Publisher]

[41] J. Yasomanee, J. Bandara, *Sol. Energy Mater. Sol. Cells.,* **2008**, *92*, 348–352. [CrossRef], [Google Scholar], [Publisher]

[42] J.R. Peller, R.L. Whitman, S. Griffith, P. Harris, C. Peller, J. Scalzitti, *J. Photochem. Photobiol. A,* **2007**, *186*, 212–217. [CrossRef], [Google Scholar], [Publisher]

[43] H. Guo, M. Kemell, M. Heikkilä, M. Leskelä, *Appl. Catal. B,* **2010**, *95*, 358–364. [CrossRef], [Google Scholar], [Publisher]

[44] N. Negishi, K. Takeuchi, T. Ibusuki, *J. Sol-Gel Sci. Technol.* **1998**, *13*, 691–694. [CrossRef], [Google Scholar], [Publisher]

[45] M.R. Elahifard, S. Rahimnejad, S. Haghighi, M.R. Gholami, *J. Am. Chem. Soc.,* **2007**, *129*, 9552–9553. [CrossRef], [Google Scholar], [Publisher]

[46] G. Liu, H. G. Yang, J. Pan, Y. Q. Yang, G. Q. Lu, H.M. Cheng, *Chem. Rev.,* **2014**, *114*, 9559–9612. [CrossRef], [Google Scholar], [Publisher]

[47] H. Sohrabi, A. Mozafari, M. Sajjadnejad, S.H. Tabaian, H. Omidvar, *Mater. Sci. Technol.,* **2016**, *32*, 1282–1288. [CrossRef], [Google Scholar], [Publisher]

[48] H. Sohrabi, S. Tabaian, H. Omidvar, M. Sajjadnejad, A. Mozafari, *Synthesis and Reactivity in Inorganic, Metal-Organic, and Nano-Metal Chemistry,* **2016**, *46*, 414–422. [CrossRef], [Google Scholar], [Publisher]

[49] S. Arman, H. Omidvar, S. Tabaian, M. Sajjadnejad, S. Fouladvand, S. Afshar, *Surface Coat. Technol.,* **2014**, *251*, 162–169. [CrossRef], [Google Scholar], [Publisher]

[50] B. Neppolian, Q. Wang, H. Yamashita, H. Choi, *Appl. Catal. A,* **2007**, *333*, 264–271. [CrossRef], [Google Scholar], [Publisher]

[51] P.D. Cozzoli, R. Comparelli, E. Fanizza, M. L. Curri, A. Agostiano, D. Laub, *J. Am. Chem. Soc.,* **2004**, *126*, 3868–3879. [CrossRef], [Google Scholar], [Publisher]

[52] J. Arbiol i Cobos, *Metal additive distribution in TiO2 and SnO2 semiconductor gas sensor nanostructured materials*. Universitat de Barcelona, **2001**. [Google Scholar], [Publisher]
[53] K. Vinodgopal, P.V. Kamat, *Environ. Sci. Technol.,* **1995**, *29*, 841–845. [CrossRef], [Google Scholar], [Publisher]
[54] C.G. Silva, A. Corma, H. García, *J. Mater. Chem.,* **2010**, *20*, 3141–3156. [CrossRef], [Google Scholar], [Publisher]
[55] M. Dan-Hardi, Serre, C., Frot, T., Rozes, L., Maurin, G., Sanchez, C. and Férey, G. *J. Am. Chem. Soc.,* **2009**, *131*, 10857–10859. [CrossRef], [Google Scholar], [Publisher]
[56] M. Alvaro, E. Carbonell, B. Ferrer, F.X. Llabrés i Xamena, H. Garcia, *Chem. Eur. J.,* **2007**, *13*, 5106–5112. [CrossRef], [Google Scholar], [Publisher]
[57] M. Allendorf, C. Bauer, R. Bhakta, R. Houk, *Chem. Soc. Rev.,* **2009**, *38*, 1330–1352. [CrossRef], [Google Scholar], [Publisher]
[58] J. Heine, K. Müller-Buschbaum, *Chem. Soc. Rev.,* **2013**, *42*, 9232–9242. [CrossRef], [Google Scholar], [Publisher]
[59] P.R. Matthes, J. Nitsch, A. Kuzmanoski, C. Feldmann, A. Steffen, T.B. Marder, K. Müller-Buschbaum, *Chem. Eur. J.,* **2013**, *19*, 17369–17378. [CrossRef], [Google Scholar], [Publisher]
[60] M. Eddaoudi, J. Kim, N. Rosi, D. Vodak, J. Wachter, M. O'Keeffe, O.M. Yaghi, *Science,* **2002**, *295*, 469–472. [CrossRef], [Google Scholar], [Publisher]
[61] J.L. Rowsell, O.M. Yaghi, *Micropor. Mesopor. Mater,* **2004**, *73*, 3–14. [CrossRef], [Google Scholar], [Publisher]
[62] S. Barman, H. Furukawa, O. Blacque, K. Venkatesan, O. M. Yaghi, H. Berke, *Chem. Commun.,* **2010**, *46*, 7981–7983. [CrossRef], [Google Scholar], [Publisher]
[63] J.R. Li, R.J. Kuppler, H.C. Zhou, *Chem. Soc. Rev.,* **2009**, *38*, 1477–1504. [CrossRef], [Google Scholar], [Publisher]
[64] J.R. Long, O.M. Yaghi, *Chem. Soc. Rev.,* **2009**, *38*, 1213–1214. [CrossRef], [Google Scholar], [Publisher]
[65] J. Lee, O.K. Farha, J. Roberts, K.A. Scheidt, S.T. Nguyen, J.T. Hupp, *Chem. Soc. Rev.,* **2009**, *38*, 1450–1459. [CrossRef], [Google Scholar], [Publisher]
[66] L. Shen, G. Wang, X. Zheng, Y. Cao, Y. Guo, K. Lin, L. Jiang, *Chinese J. Catal.,* **2017**, *38*, 1373–1381, [CrossRef], [Google Scholar], [Publisher]
[67] A. Dhakshinamoorthy, M. Alvaro, H. Garcia, *Chem. Commun.,* **2012**, *48*, 11275–11288. [CrossRef], [Google Scholar], [Publisher]
[68] B.M. Rajbongshi, S. Samdarshi, *Appl. Catal. B,* **2014**, *144*, 435–441. [CrossRef], [Google Scholar], [Publisher]
[69] J. Gascon, M.D. Hernández-Alonso, A.R. Almeida, G.P. van Klink, F. Kapteijn, G. Mul, *Chem. Sus. Chem.,* **2008**, *1*, 981–983. [CrossRef], [Google Scholar], [Publisher]
[70] W. Jiang, Y. Zhou, H. Geng, S. Jiang, S. Yan, W. Hu, Z. Wang, , Z. Shuai, J. Pei, *J. Am. Chem. Soc.,* **2010**, *133*, 1–3. [CrossRef], [Google Scholar], [Publisher]
[71] K.K. Tanabe, C.A. Allen, S.M. Cohen, *Angew. Chem., Int. Ed.,* **2010**, *49*, 9730–9733. [CrossRef], [Google Scholar], [Publisher]
[72] A. Modrow, D. Zargarani, R. Herges, N. Stock, *Dalton Trans.,* **2011,** *40*, 4217–4222. [CrossRef], [Google Scholar], [Publisher]
[73] A. Michaelides, S. Skoulika, M.G. Siskos, *Chem. Commun.,* **2011**, *47*, 7140–7142. [CrossRef], [Google Scholar], [Publisher]
[74] F.X. Llabrés i Xamena, A. Corma, H. Garcia, *J. Phys. Chem. C,* **2007**, *111*, 80–85. [CrossRef], [Google Scholar], [Publisher]
[75] P. George, N.R. Dhabarde, P. Chowdhury, *Mater. Lett.,* **2017**, *186*, 151–154. [CrossRef], [Google Scholar], [Publisher]
[76] C. Gomes Silva, I. Luz, F. X. Llabrés i Xamena, A. Corma, H. García, *Chem. Eur. J.,* **2010**, *16*, 11133–11138. [CrossRef], [Google Scholar], [Publisher]

[77] S. Pu, L. Xu, L. Sun, H. Du, *Inorg. Chem. Commun.,* **2015,** *52*, 50–52. [CrossRef], [Google Scholar], [Publisher]

[78] H.P. Jing, C.C. Wang, Y.W. Zhang, P. Wang, R. Li, *RSC Adv.,* **2014,** *4*, 54454–54462. [CrossRef], [Google Scholar], [Publisher]

[79] Y. Fu, D. Sun, Y. Chen, R. Huang, Z. Ding, X. Fu, Z.Li, *Angew. Chem., Int. Ed.,* **2012,** *51*, 3364–3367. [CrossRef], [Google Scholar], [Publisher]

[80] T. Zhang, W. Lin, *Chem. Soc. Rev.,* **2014**, *43*, 5982–5993. [CrossRef], [Google Scholar], [Publisher]

[81] S. Mosleh, M. Rahimi, M. Ghaedi, K. Dashtian, S. Hajati, *RSC Adv.,* **2016**, *6*, 17204–17214. [CrossRef], [Google Scholar], [Publisher]

[82] D. Wang, J. Albero, H. García, Z. Li, *J. Catal.,* **2017,** *349*, 156–162. [CrossRef], [Google Scholar], [Publisher]

[83] H. Ramezanalizadeh, F. Manteghi, *J. Clean. Prod.,* **2018**, *172*, 2655–2666, [CrossRef], [Google Scholar], [Publisher]

[84] S.R. Thakare, S.M. Ramteke, *J. Phys. Chem. Solid.,* **2018,** *116*, 264–272. [CrossRef], [Google Scholar], [Publisher]

[85] A. Crake, K.C. Christoforidis, A. Kafizas, S. Zafeiratos, C. Petit, *Appl. Catal. B,* **2017,** *210*, 131–140. [CrossRef], [Google Scholar], [Publisher]

[86] N.M. Mahmoodi, J. Abdi, *Microchem. J.,* **2019,** *144*, 436–442. [CrossRef], [Google Scholar], [Publisher]

[87] C. Jing, Y. Zhang, J. Zheng, S. Ge, J. Lin, D. Pan, N. Naik, Z. Guo, *Particuology,* **2022,** *69*, 111–122. [CrossRef], [Google Scholar], [Publisher]

[88] Z. Durmus, R. Köferstein, T. Lindenberg, F. Lehmann, D. Hinderberger, A.W. Maijenburg, *Ceram. Int.,* **2023**, *In Press.* [CrossRef], [Google Scholar], [Publisher]

[89] J. Qiu, X. Zhang, Y. Feng, X. Zhang, H. Wang, J. Yao, *Appl. Catal. B,* **2018**, *231*, 317–342. [CrossRef], [Google Scholar], [Publisher]

[90] T. Tachikawa, J. R. Choi, M. Fujitsuka, T. Majima, *J. Phys. Chem. C,* **2008,** *112*, 14090–14101. [CrossRef], [Google Scholar], [Publisher]

[91] M.C. Das, H. Xu, Z. Wang, G. Srinivas, W. Zhou, Y.F. Yue, V.N. Nesterov, G. Qian, B. Chen, *Chem. Commun.,* **2011,** *47*, 11715–11717. [CrossRef], [Google Scholar], [Publisher]

[92] K. Laurier, F. Vermoortele, R. Ameloot, D. De Vos, J. Hofkens, and M. Roeffaers, *J. Am. Chem. Soc.,* **2013,** *135*, 14488–14491. [CrossRef], [Google Scholar], [Publisher]

[93] L. Chi, Q. Xu, X. Liang, J. Wang, X. Su, *Small,* **2016**, *12*, 1351–1358. [CrossRef], [Google Scholar], [Publisher]

[94] J. Gao, J. Miao, P.Z. Li, W.Y. Teng, L. Yang, Y. Zhao, B. Liu, Q. Zhang, *Chem. Commun.,* **2014**, *50*, 3786–3788. [CrossRef], [Google Scholar], [Publisher]

[95] D. Wang, M. Wang, Z. Li, *ACS Catal.,* **2015,** *5*, 6852–6857. [CrossRef], [Google Scholar], [Publisher]

[96] R. Liang, F. Jing, L. Shen, N. Qin, L. Wu, *J. Hazard. Mater.,* **2015**, *287*, 364–372. [CrossRef], [Google Scholar], [Publisher]

[97] C. Zhang, L. Ai, J. Jiang, *J. Mater. Chem. A,* **2015**, *3*, 3074–3081. [CrossRef], [Google Scholar], [Publisher]

[98] Y. Gao, S. Li, Y. Li, L. Yao, H. Zhang, *Appl. Catal. B,* **2017**, *202*, 165–174. [CrossRef], [Google Scholar], [Publisher]

[99] B. Pattengale, S. Yang, J. Ludwig, Z. Huang, X. Zhang, J. Huang, *J. Am. Chem. Soc.,* **2016**, *138*, 8072–8075. [CrossRef], [Google Scholar], [Publisher]

[100] H. Park, D.A. Reddy, Y. Kim, R. Ma, J. Choi, T.K. Kim, K.S. Lee, *Solid State Sci.,* **2016**, *62*, 82–89. [CrossRef], [Google Scholar], [Publisher]

[101] E.A. Kozlova, V.N. Panchenko, Z. Hasan, N. A. Khan, M.N. Timofeeva, S.H. Jhung, *Catal. Today,* **2016**, *266*, 136–143. [CrossRef], [Google Scholar], [Publisher]

HOW TO CITE THIS ARTICLE

Mohammad Sajjadnejad *, Seyyed Mohammad Saleh Haghshenas. Metal Organic Frameworks (MOFs) and their Application as Photocatalysts: Part II. Characterization and Photocatalytic Behavior. *Adv. J. Chem. A*, **2023**, 6(2), 172-187. **DOI: 10.22034/AJCA.2023.389622.1357 URL: http://www.ajchem-a.com/article_169946.html**